Nuclear Export of the NF-κB Inhibitor IκBα Is Required for Proper B Cell and Secondary Lymphoid Tissue Formation

Shelly M. Wuerzberger-Davis,[1,8] Yuhong Chen,[2,8] David T. Yang,[3] Jeffrey D. Kearns,[4] Paul W. Bates,[1,9] Candace Lynch,[4] Nicholas C. Ladell,[1] Mei Yu,[2,5] Andrew Podd,[2,6] Hu Zeng,[2,5] Tony T. Huang,[7] Renren Wen,[2] Alexander Hoffmann,[4] Demin Wang,[2,5,6,*] and Shigeki Miyamoto[1,*]

[1]McArdle Laboratory for Cancer Research, Department of Oncology, University of Wisconsin Carbone Cancer Center, University of Wisconsin-Madison, 6159 Wisconsin Institute for Medical Research, 1111 Highland Avenue, Madison, WI 53705, USA
[2]Blood Research Institute, BloodCenter of Wisconsin, Milwaukee, WI 53226, USA
[3]Department of Pathology and Laboratory Medicine, University of Wisconsin-Madison, B4/259 Clinical Sciences Center, 600 Highland Avenue, Madison, WI 53792, USA
[4]Signaling Systems Laboratory, Department of Chemistry and Biochemistry, University of California, San Diego, 9500 Gilman Drive, La Jolla, CA 92093, USA
[5]State Key Laboratory of Pharmaceutical Biotechnology, College of Life Science, Nanjing University, Nanjing 210093, P. R. China
[6]Department of Microbiology and Molecular Genetics, Medical College of Wisconsin, Milwaukee, WI 53226, USA
[7]Department of Biochemistry, New York University, New York, NY 10016, USA
[8]These authors contributed equally to this work
[9]Present address: Department of Biology, University of Minnesota, Duluth, MN 55812, USA
*Correspondence: demin.wang@bcw.edu (D.W.), smiyamot@wisc.edu (S.M.)
DOI 10.1016/j.immuni.2011.01.014

SUMMARY

The N-terminal nuclear export sequence (NES) of inhibitor of nuclear factor kappa B (NF-κB) alpha (IκBα) promotes NF-κB export from the cell nucleus to the cytoplasm, but the physiological role of this export regulation remains unknown. Here we report the derivation and analysis of genetically targeted mice harboring a germline mutation in IκBα NES. Mature B cells in the mutant mice displayed nuclear accumulation of inactive IκBα complexes containing a NF-κB family member, cRel, causing their spatial separation from the cytoplasmic IκB kinase. This resulted in severe reductions in constitutive and canonical NF-κB activities, synthesis of p100 and RelB NF-κB members, noncanonical NF-κB activity, NF-κB target gene induction, and proliferation and survival responses in B cells. Consequently, mice displayed defective B cell maturation, antibody production, and formation of secondary lymphoid organs and tissues. Thus, IκBα nuclear export is essential to maintain constitutive, canonical, and noncanonical NF-κB activation potentials in mature B cells in vivo.

INTRODUCTION

The NF-κB-Rel family of transcription factors regulates multiple physiologic processes, including innate and adaptive immunity and various stress responses (Ghosh and Hayden, 2008; Perkins, 2007). In mammals, this consists of five members, RelA (p65), cRel, RelB, NFkB1 (p50), and NFkB2 (p52), which form dimers, such as the most widely expressed RelA:p50 or more tissue-restricted cRel homo- and heterodimers. A key feature of NF-κB dimers is their cytoplasmic localization as inactive complexes while bound to members of the inhibitor of NF-κB (IκB) family, such as IκBα and IκBβ. Activation of NF-κB requires its release from IκB to allow nuclear migration and target gene regulation. "Canonical" activation involves the activation of the cytoplasmic IκB kinase (IKK) complex composed of IKKα (IKK1), IKKβ (IKK2), and IKKγ (NF-κB essential modulator, NEMO) that induces phosphorylation-regulated degradation of IκB, releasing NF-κB dimers to the nucleus. This activation pathway is induced by a variety of extracellular stimuli or stress conditions and is principle in many NF-κB activation processes (Ghosh and Hayden, 2008; Perkins, 2007). An alternative "noncanonical" pathway exists, where the precursor of p52, p100, is phosphorylated by the IKKα complex, without the need for IKKβ and NEMO. After phosphorylation, p100 is processed to selectively activate a RelB:p52 heterodimer in response to specific inducers. RelB:p52 complexes do not associate with canonical IκB proteins and therefore are not directly regulated by them. The noncanonical pathway is critical for lymphoid organ development and immune cell development, among others (Hoffmann and Baltimore, 2006; Sen, 2006).

Classically, IκB is thought to mask the nuclear localization sequence (NLS) of RelA to prevent its nuclear entry, thereby "sequestering" NF-κB in the cytoplasm (Baeuerle and Baltimore, 1988). This mode of regulation appears to be the case for complexes containing IκBβ (Huang et al., 2000; Malek et al., 2001; Tam et al., 2001). However, studies employing the nuclear export inhibitor leptomycin B (LMB) provide contrasting evidence that RelA:IκBα, cRel:IκBα, and RelA:IκBε complexes shuttle between the cytoplasm and the nucleus in their inactive state (Carlotti et al., 2000; Huang et al., 2000; Johnson et al.,

1999; Malek et al., 2001; Tam et al., 2000). In support of this dynamic "nucleocytoplasmic shuttling" model, RelA:p50:IκBα cocrystal structures indicate that IκBα masks the NLS of RelA but spares that of p50 (Huxford et al., 1998). Moreover, p50 NLS is found to be critical for nuclear import of RelA:p50:IκBα complexes (Huang et al., 2000; Malek et al., 2001; Tam et al., 2001). An alternative model has also been implicated in which NF-κB and IκBα complexes enter the nucleus separately but exit together (Carlotti et al., 2000; Tam et al., 2000). The mechanism of nuclear export of the complexes also appears intricate, possibly involving multiple distinct nuclear export sequences (NESs) present on IκBα, IκBε, and RelA (Huang et al., 2000; Johnson et al., 1999; Malek et al., 2001; Tam et al., 2000). Interestingly, other NF-κB family members, such as cRel and p50, do not contain NES motifs in their sequences, suggesting that their export depends on a nuclear export function provided primarily by IκBα. However, these studies employed cell culture models often utilizing LMB and/or transient overexpression of respective proteins, so the physiological importance of this NES-mediated shuttling mechanism has been questioned (Ghosh and Karin, 2002). Indeed, there has not been any direct in vivo study to evaluate the physiological role of nuclear export of any of the NF-κB:IκB complexes and mechanisms implicated.

To address this question, we created a genetically targeted mouse model harboring a germline mutation in the N-terminal NES of IκBα (Huang et al., 2000). Here, we have described the mechanistic and phenotypic characterization of the mutant mice and cells derived from them. Our results reveal a surprising finding that the nuclear export function mediated by IκBα N-NES is essential for basal, canonical, and noncanonical NF-κB activation in B lymphocytes, maturation of B cells, and formation of several secondary lymphoid tissues. Our study reveals insight into important physiological and cell type-selective functions of nuclear export regulation of the NF-κB-IκB signaling system in vivo.

RESULTS

Generation of *Nfkbia*[NES/NES] Genetically Targeted Mice

We created *Nfkbia*[NES/NES] mice harboring a triple point mutation in the N-terminal NES of IκBα, M45A, L49A, and I52A (Huang et al., 2000) in the germline (Figures S1A and S1B available online). The heterozygous *Nfkbia*[+/NES] mice were backcrossed with C57BL/6J mice for 5–7 generations. Homozygous mutant mice were also bred to each other. These studies demonstrated that both male and female *Nfkbia*[NES/NES] mice were born in a Mendelian ratio, fertile, and indistinguishable from their wild-type (WT) counterparts based on size, weight, or general appearance at sexual maturity (not shown). Allele-specific RT-PCR analysis of total RNA (Figure S1C) and immunoblot analysis of total protein extracts from several tissues (Figure S1D) demonstrated the expression of the mutant gene and the protein in *Nfkbia*[NES/NES] mice. The migration of the mutant protein in sodium dodecyl sulfate polyacrylamide gel electrophoresis was partially retarded compared to WT protein (Figure S1D), a phenomenon also observed when the protein was transiently expressed in HEK293 cells (not shown). This suggests that the property is an intrinsic migration anomaly resulting from the substitution mutations introduced.

Abnormal Formation of Secondary Lymphoid Organs and Tissues in *Nfkbia*[NES/NES] Mice

A closer inspection revealed that the inguinal lymph nodes were often bilaterally absent in the mutant mice (Figure 1A) and, when present, they were considerably smaller and showed disrupted B cell organization (Figures 1B and 1C). Therefore, we next examined other lymphoid tissues and organs more closely. Although other lymph nodes analyzed (cervical, mesenteric, and lumber) were comparable to WT numbers, intestine-associated Peyer's patches, mucosal lymphoid organs involved in protection from intestinal microbes as well as production of IgA, were markedly reduced in number and size in the mutant mice (Figures 1D and 1E). Finally, although the size and weight of spleens were indistinguishable between WT and mutant littermates, the organization of B cells and marginal zone (MZ) architecture were also disrupted in the spleen of the mutant mice (Figures 1F and 1G). In contrast, based on morphology, weight, and histology, the thymus was indistinguishable between WT and mutant mice (Figure 1H and data not shown). Thus, IκBα N-NES is essential for proper formation of several secondary lymphoid organs and tissues.

Impaired Maturation of B Cells in *Nfkbia*[NES/NES] Mice

We next assessed the development and maturation of lymphocytes in the bone marrow (BM), spleen, and thymus of *Nfkbia*[NES/NES] mice based on cell surface marker expression (Hardy and Hayakawa, 2001). An expanded population of pre-B cells (B220^{+}CD43^{−}IgM^{−}) was observed in mutant mice leading to slightly increased BM B cell numbers, but overall total BM cell numbers were comparable between WT and mutant mice (Figures S2A–S2D). Despite the increase in the absolute number of immature B cells (B220[+]IgM[+]) in *Nfkbia*[NES/NES] mice, the population of mature B cells (B220[hi]IgM[+]) in BM was decreased (Figures S2B and S2D). In the spleen, the percentage of T cells was increased and that of B cells was decreased (Figure 2A), but the number of total Thy1.2^{+} (Figure 2B) or CD4^{+} and CD8^{+} T cells in the spleen was similar in *Nfkbia*[NES/NES] mice (Table 1). Similarly, thymic T cell development was indistinguishable between mutant and WT mice based on CD4 and CD8 staining (Figures 2C and 2D). The difference in the percentage of T and B cells in the spleen was due to the reduction of the number of B220^{+} B cells (Figure 2B), involving reductions of the transitional 2 (T2) and follicular (FO), but not transitional 1 (T1) B cell fractions (Figures 2E, 2F, and 2I). The MZ B cells (Oliver et al., 1997) were also decreased (Figures 2F–2I). Additionally, the self-renewing mature B1a and B1b B cells that reside in the peritoneal and pleural cavities (Fagarasan et al., 2000) were largely normal but the population of peritoneal B2 B cells was substantially reduced in *Nfkbia*[NES/NES] mice (Figures S2E and S2F). Finally, there was a statistically significant reduction of serum IgA, IgG1, and IgG2b amounts in the mutant mice (Figure 2J). Taken together, we conclude that the NES mutation in IκBα impairs B cell maturation, resulting in reduction of T2, FO, and MZ B cells. Moreover, the failure of BM cells derived from *Nfkbia*[NES/NES] mice to properly reconstitute T2, FO, and MZ B cells in irradiated B cell-null *Jak3*^{−/−} (Figures 3A–3D; Nosaka et al., 1995; Thomis et al., 1995) or *Rag2*^{−/−} (not shown) mice demonstrated that these B cell defects in *Nfkbia*[NES/NES] mice were hematopoietically cell intrinsic. The above phenotypes observed in
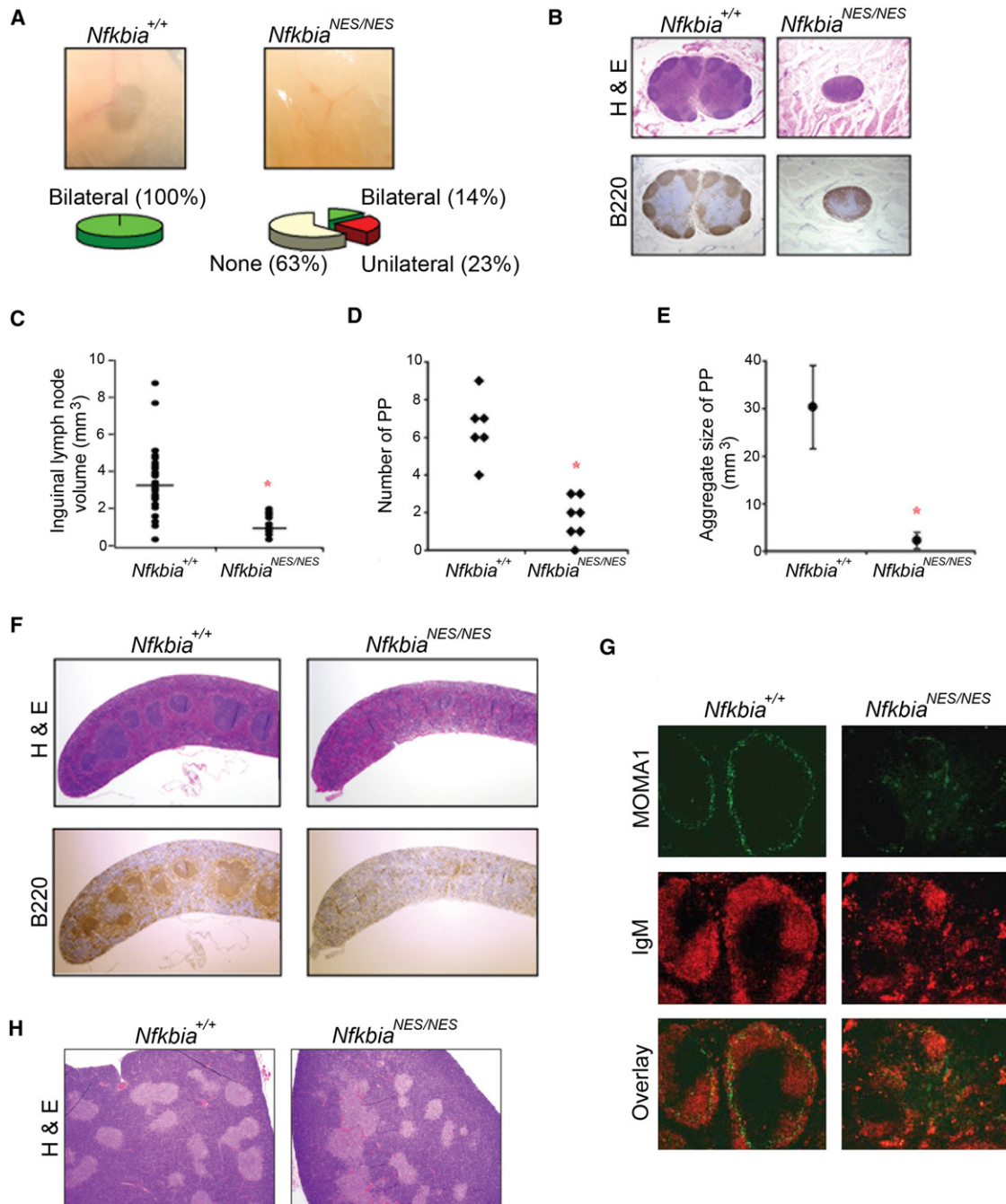
Figure 1. Defects of Proper Formation of Spleen, Inguinal LNs, and PPs in *Nfkbia*^{NES/NES} Mice

(A) Photographs of inguinal LNs in situ from WT and *Nfkbia*^NES/NES^ littermates (top). LNs were counted in WT (n = 35) and *Nfkbia*^NES/NES^ (n = 35) mice and displayed graphically (bottom).

(B) Inguinal LNs in WT and *Nfkbia*^NES/NES^ mice were analyzed by hematoxylin and eosin (H&E) stain and immunostaining with anti-B220.

(C) Inguinal LN volume was derived by the formula width^2 × length/2 of histologic sections from wild-type (n = 32) and *Nfkbia*^NES/NES^ (n = 11) mice and displayed graphically. The difference is statistically significant (*p < 0.001, unpaired t test).

(D) PPs were counted from WT (n = 6) and *Nfkbia*^NES/NES^ (n = 7) mice and displayed graphically.

(E) Aggregate size of PPs were calculated as in (C) from samples in (D). Data are mean ± SD, *p < 0.001 versus WT.

(F) Spleens from WT and *Nfkbia*^NES/NES^ mice were analyzed by H&E stain and immunostaining with anti-B220, 4× objective.

(G) Immunofluorescent histochemical analysis of the spleens from WT or *Nfkbia*^NES/NES^ mice were analyzed with anti-MOMA-1 and anti-IgM. MZ B cell layer is external to the ring of metallophilic macrophages.

(H) Thymii from WT or *Nfkbia*^NES/NES^ mice were analyzed by H&E stain, 4× objective.

Nfkbia$^{NES/NES}$ mice were also detected at variable amounts in heterozygous *Nfkbia*$^{+/NES}$ mice (Table 1), demonstrating that a single copy of the mutant allele had a variably dominant impact on these biological processes.

Diminished Constitutive and Canonical Activation of NF-κB in *Nfkbia*$^{NES/NES}$ B Cells

To determine whether NF-κB activation was affected in B cells of the mutant mice, we isolated splenic B cells and performed electrophoretic mobility shift assays (EMSA) and supershift analyses. We found that a constitutive NF-κB complex primarily composed of cRel and p50 or p52 (Figure 4A, upper complex) was severely reduced in *Nfkbia*$^{NES/NES}$ B cells compared to WT cells. When these B cells were exposed to anti-IgM to stimulate B cell receptor signaling, we also observed activation defects (Figure 4B). Similarly, mutant B cells were incapable of efficiently activating NF-κB in response to lipopolysaccharide (LPS) (Figure 4C), demonstrating that mutant B cells were defective in canonical NF-κB activation. Anti-IgM- and LPS-induced degradation of IκBα was less efficient in mutant B cells (Figures 4D and 4E), despite similar IKK activation as observed after LPS stimulation (Figure 4F) in WT and *Nfkbia*$^{NES/NES}$ B cells. IκBβ degradation appeared to be induced at comparable amounts (Figures 4D and 4E). When we examined the subcellular localization of IκBα by immunofluorescence analysis, it was predominantly localized in the nucleus in mutant B cells (Figures 4G–4I). Similarly, more cRel was found in the nucleus (Figures 4G–4I) even though it did not bind DNA (Figure 4A). Coimmunoprecipitation analysis showed that IκBα was associated with cRel (Figure 4J). We were unable to obtain similarly high nuclear IκBα and cRel amounts in mutant B cells by a cell fractionation approach, probably because of technical limitations (Figure S3A). In total, the results suggest that spatial separation between active cytoplasmic IKK and nuclear inactive cRel:IκBα complexes prevented efficient canonical NF-κB activation in *Nfkbia*$^{NES/NES}$ B cells. Interestingly, RelA subcellular localization was perturbed to a much smaller extent in B cells (Figures S3B and S3C), possibly because of the presence of a compensatory NES in RelA (Harhaj and Sun, 1999; Tam et al., 2001).

Defective Noncanonical NF-κB Activation in *Nfkbia*$^{NES/NES}$ B Cells

In the above coimmunoprecipitation analysis, we noted that the steady-state amount of cRel was reduced in mutant B cells compared to WT cells (Figure 4J). The expression of the genes encoding several NF-κB family members is controlled by NF-κB in B cells because of the presence of κB elements in their promoters (Grumont and Gerondakis, 1994; Perkins, 2007). Accordingly, expression of cRel, RelB, p105 (p50), and p100 (p52) in the mutant B cells was reduced compared to the WT littermate control (Figure 5A). Expression of RelA in mutant B cells was also slightly reduced. Quantitative real-time polymerase chain reaction analysis showed that amounts of transcripts encoding cRel, RelB, and p100 (p52) were considerably lower in the *Nfkbia*$^{NES/NES}$ B cells (Figure 5B). Moreover, although the transcript of the mutant *Nfkbia* gene was not statistically significantly different (not shown), the amount of mutant IκBα protein was higher in mutant B cells (Figures 4D, 4E, 4J, and 5A). This was also evident in *Nfkbia*$^{+/NES}$ B cells (Figure 5A).

This is due to higher stability of mutant IκBα protein (Figure 5C), consistent with its resistance to signal-induced degradation (Figures 4D and 4E). The relative stability of the mutant IκBα would lead to a greater steady-state pool of the mutant as compared to WT IκBα. This could explain why *Nfkbia*$^{+/NES}$ mice also had considerable defects in B cell maturation and development of lymph nodes and Peyer's patches (Table 1), functioning as a dominant-suppressive IκBα mutant protein in vivo. Finally, IκBβ was slightly reduced in the mutant B cells (Figures 4D, 4E, 4J, and 5A), possibly reflecting the reduced expression of its partner NF-κB proteins in these cells. Although B cell activating factor-receptor (BAFF-R) expression was normal (Figure S4A) and BAFF-induced p100 processing was evident (Figure 5D), there was a severe defect in activation of BAFF-induced noncanonical NF-κB activation containing RelB (Figure S4B) in *Nfkbia*$^{NES/NES}$ B cells (Figure 5E). In contrast, basal expression of p100 and all other NF-κB family members was similar between mouse embryonic fibroblasts (MEFs) derived from *Nfkbia*$^{NES/NES}$ and WT littermate controls (Figure 5F; Figure S4C). Noncanonical NF-κB activity induced by anti-lymphotoxin beta (LTβ) was also similar in these cells (Figure 5G). Canonical activation induced by tumor necrosis factor alpha (TNF-α) or LPS was also mostly normal in MEFs derived from *Nfkbia*$^{NES/NES}$ mice (Figure S4D). Thus, the reduced basal NF-κB family member expression and canonical and noncanonical NF-κB activation defects seen in mutant B cells were cell type-selective phenotypes. This was associated with a marked reduction in constitutive activation of cRel complexes along with constitutive nuclear cRel:IκBα complexes that were resistant to signal-induced activation in mature B cells. Taken together, these results demonstrate that a nuclear export defect in IκBα caused large-scale perturbations in the capacity of B cells to maintain NF-κB activation potentials through constitutive, canonical, and noncanonical pathways.

Defective Proliferation and Survival in *Nfkbia*$^{NES/NES}$ B Cells

Deficiencies in canonical and noncanonical NF-κB activation are associated with cellular proliferation and apoptosis defects in B cells (Ghosh and Hayden, 2008; Vallabhapurapu and Karin, 2009). Consistent with severe canonical and noncanonical NF-κB activation defects, we found that B cells (both AA4.1$^+$ immature and AA4.1$^-$ mature) from *Nfkbia*$^{NES/NES}$ mice displayed reduced proliferation rates compared to WT cells (Figures 6A and 6B). This correlated with reduced entry of *Nfkbia*$^{NES/NES}$ B cells into S and G$_2$-M phases upon anti-IgM+interleukin-4 (IL-4) or LPS stimulation (Figures 6C and 6D). Upon stimulation, more mature B cells from *Nfkbia*$^{NES/NES}$ mice underwent apoptosis than those from WT cells (Figure 6D). Accordingly, expression of *Myc* and *Bcl2l1* (encoding protein BCLx$_L$), both NF-κB target genes involved in proliferation and survival, respectively, was markedly reduced in mutant B cells (Figures 6E and 6F). Thus, IκBα N-NES is also critical for B cell proliferation and survival. In contrast, proliferation of thymic and splenic T cells from both WT and *Nfkbia*$^{NES/NES}$ mice in response to anti-CD3, anti-CD3+anti-CD28, or anti-CD3+IL-2 was indistinguishable (Figure 6G). Subcellular localization of mutant IκBα in *Nfkbia*$^{NES/NES}$ T cells was mostly normal in association with cytoplasmic RelA (Figures S5A and S5B). A flurry of recent reports
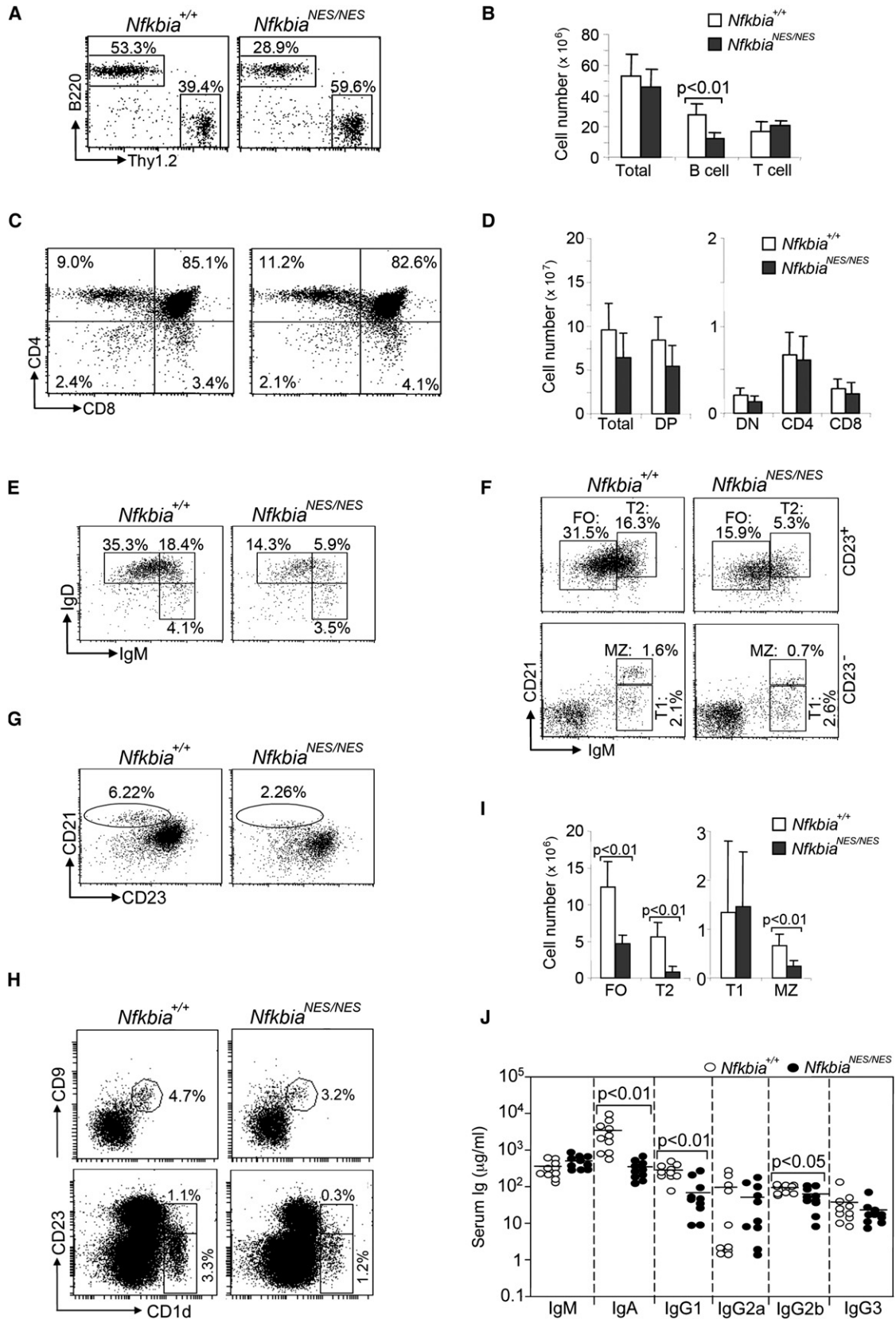
demonstrates that cRel plays an essential role in the development of regulatory T cells by promoting *Foxp3* transcription (Deenick et al., 2010; Hori, 2010; Isomura et al., 2009; Long et al., 2009; Ruan et al., 2009; Vang et al., 2010; Visekruna et al., 2010; Zheng et al., 2010), so we also investigated whether regulatory T cells were affected in the mutant mice. Analysis of a limited number of WT and *Nfkbia*[NES/NES] mice showed statistically significant developmental defects of this cell type in the mutant mice (Figures S5C and S5D). Similarly, cRel and p50 have also been implicated in the development of CD4^{+} memory-like T cells (Zeng et al., 2008; Zheng et al., 2003). Likewise, we also found statistically significant reductions of CD4^{+}, but not CD8^{+}, memory-like T cells in the mutant mice (Figures S5E and S5F). Thus, in these T cell subsets, cRel activities are probably disrupted in the *Nfkbia*[NES/NES] mice. Overall, our data demonstrate that a defect in the IκBα N-NES function causes multiple unexpected biochemical and functional perturbations in mature B cells and subsets of T cells and malformation of multiple secondary lymphoid tissues and organs.

DISCUSSION

In the present study, we demonstrated that IκBα N-NES-mediated export of NF-κB has important physiological roles, particularly for maturation of B cells and proper formation of several secondary lymphoid organs and tissues. The primary molecular defect appears to be the abnormal nuclear localization of inactive cRel:IκBα complexes, which makes them resistant to signal-induced IκBα degradation and cRel complex activation in *Nfkbia*[NES/NES] B cells. Because the mutant protein accumulates over the WT protein (because of its resistance to degradation), it also functions as a dominant-suppressive mutant causing heterozygous *Nfkbia*[+/NES] mice to similarly show significant in vivo defects. Consistent with these findings, some of the phenotypes observed in *Nfkbia*[NES/NES] mice were reminiscent of those previously described in *Rel*^{−/−} mice, such as reduced proliferation of splenic B cells and a reduction of serum IgG1 (Köntgen et al., 1995). Furthermore, *Nfkbia*[NES/NES] mice also displayed reductions in FO and MZ B cell populations and serum IgA previously observed in *Rel*^{−/−}*Nfkb1*^{−/−} double-mutant mice (Pohl et al., 2002). In contrast, *Nfkbia*[NES/NES] mice showed normal peritoneal B1 B cell development, unlike *Rel*^{−/−}*Nfkb1*^{−/−}

mice (Pohl et al., 2002). It is likely that the amount of inhibition of cRel:p50 activity or other cRel-associated complexes is not sufficiently inhibited in B1 B cells of *Nfkbia*[NES/NES] mice to yield profound defects observed in *Rel*^{−/−}*Nfkb1*^{−/−} mice.

We also observed severe defects in noncanonical NF-κB activation in *Nfkbia*[NES/NES] B cells. This was a surprising finding because IκBα does not bind RelB:p52 heterodimers and therefore it cannot directly inhibit noncanonical NF-κB activity. Accordingly, BAFF-induced p100 processing to p52 could be readily detected, indicating that the noncanonical signaling pathway per se is not defective in *Nfkbia*[NES/NES] B cells. Moreover, the noncanonical activation defect was specific to mutant B cells, because we did not find any defect in LTβR-induced noncanonical p100 processing or RelB:p52 activation in *Nfkbia*[NES/NES] MEFs. Instead, our data indicate that the noncanonical activation defects in *Nfkbia*[NES/NES] B cells arose from the reduced transcripts for *Nfkb2* and *Relb* genes and resulting reductions in their encoded noncanonical NF-κB proteins. Ferch et al. (2007) recently reported that B cell receptor (BCR) signaling induces Bcl10- and MALT1-dependent cRel activation whereas Bcl10, but not MALT1, is involved in RelA activation, thereby separating the mechanism of these canonical complex activation pathways. In addition, Stadanlick et al. (2008) and Castro et al. (2009) also reported that "tonic" BCR-stimulated NF-κB activity during B cell maturation promotes the de novo production of cRel. They further showed that this cRel synthesis is required for sustained cRel activity and de novo p100 synthesis, which permitted BAFF (BLyS)-mediated noncanonical RelB:p52 activation and B cell survival. Consistent with these reports, severe defects in constitutive (or tonic) and anti-IgM-induced cRel complex activity observed in mature *Nfkbia*[NES/NES] B cells are associated with reduced expression of *Rel* and *Nfkb2* genes and proteins. Moreover, we further found that expression of *Relb* mRNA and protein was also considerably reduced in mature *Nfkbia*[NES/NES] B cells. Transcription of *Rel*, *Nfkb2*, and *Relb* (as well as *Nfkb1*) is controlled by NF-κB in B cells (Castro et al., 2009; Grumont and Gerondakis, 1994; Perkins, 2007). Thus, nuclear export of IκBα is required for tonic (or constitutive) and sustained cRel activation, cRel-mediated synthesis of noncanonical NF-κB components, p100 and RelB, and the crosstalk between canonical and noncanonical NF-κB pathways in mature B cells. Defects in agonist-induced proliferation and apoptosis,

---

Figure 2. Severely Impaired B Cell Maturation in *Nfkbia*[NES/NES] Mice
Comparisons between WT and *Nfkbia*[NES/NES] mice are shown in each panel.
(A) Splenocytes were stained with anti-B220 and anti-Thy1.2. Percentages above each box indicate cells in the gated lymphoid population.
(B) The numbers of total splenocytes and total splenic B and T cells are displayed graphically.
(C) Thymocytes from WT and *Nfkbia*[NES/NES] mice were stained with anti-CD4 and anti-CD8. Percentages indicate cells in the gated lymphoid population (C and E–G).
(D) The numbers of total thymocytes and DN, DP, CD4^{+}, and CD8^{+} T cells in the thymus of WT and *Nfkbia*[NES/NES] mice are displayed graphically.
(E) Splenocytes were stained with anti-B220, anti-IgM, and anti-IgD. For cells gated on B220[+], T1 (IgM[hi]IgD[−]), T2 (IgM^{hi}IgD^{+}), and FO (IgM^{lo}IgD^{+}) B cells are shown.
(F) Splenocytes were stained with anti-IgM, anti-CD21, and anti-CD23. For cells gated on CD23^{+}, T2 (CD21^{hi}IgM^{hi}) and FO (CD21^{int}IgM^{lo}) B cells are shown. For cells gated on CD23^{−}, T1 (CD21^{lo}IgM^{hi}) and MZ (CD21^{hi}IgM^{hi}) B cells are shown.
(G) Splenocytes were stained with anti-B220, anti-CD21, and anti-CD23. For cells gated on B220^{+}, MZ B cells (CD21^{hi}CD23^{lo}) are shown.
(H) Top: Splenocytes were stained with anti-B220, anti-CD1d, and anti-CD9. For cells gated on B220^{+}, MZ (CD1d^{+}CD9^{+}) cells are shown. Bottom: Splenocytes were stained with anti-IgM, anti-CD1d, and anti-CD23. For gated lymphoid cells, T2 (CD1d^{+}CD23^{+}) and MZ (CD1d^{+}CD23^{−}) cells are shown.
(I) The numbers of T1, T2, FO, and MZ B cells obtained from (F) are displayed graphically.
(J) Serum Ig amounts were determined by ELISA. The mean value and standard deviation of the serum Ig amounts were calculated.
Data shown are representative of or obtained from 7 (A–G, I), 2 (H), or 10 (J) mice of each genotype.

Table 1. Summary of Defects Seen in *Nfkbia*$^{+/NES}$ and *Nfkbia*$^{NES/NES}$ Mice

Phenotypes	*Nfkbia*$^{+/+}$	*Nfkbia*$^{+/NES}$	*Nfkbia*$^{NES/NES}$
B Cells (×10^6)			
Bone marrow (6)			
Total B	9.3 ± 1.1	12.1 ± 2.5	11.7 ± 2.3
Pro pre-B	4.2 ± 0.7	6.8 ± 1.5**	7.3 ± 1.3**
Immature B	1.3 ± 0.2	2.1 ± 1.0	2.0 ± 0.8
Mature B	2.6 ± 0.4	2.0 ± 0.5	1.3 ± 0.4**
Spleen (7)			
Total B	26.6 ± 7.1	14.9 ± 2.6**	12.9 ± 3.3**
Transitional T1	1.3 ± 1.5	1.3 ± 0.7	1.5 ± 1.1
Transitional T2	5.7 ± 2.0	1.9 ± 1.1**	0.8 ± 0.7**
Follicular	12.4 ± 3.4	7.8 ± 2.0**	4.7 ± 1.3**
Marginal zone	0.7 ± 0.2	0.3 ± 0.2**	0.2 ± 0.1**
Lymph nodes (4)			
Total B	1.0 ± 0.5	0.3 ± 0.1*	0.2 ± 0.1*
T Cells (×10^6)			
Thymus (7)			
Total T	95.6 ± 30.1	84.7 ± 26.0	64.6 ± 26.3
CD4$^-$CD8$^-$	2.0 ± 0.8	1.5 ± 0.4	1.3 ± 0.6
CD4$^+$CD8$^+$	83.7 ± 25.9	73.6 ± 23.6	54.8 ± 21.9
CD4$^+$CD8$^-$	6.7 ± 2.5	6.7 ± 1.6	6.0 ± 2.7
CD4$^-$CD8$^+$	2.8 ± 1.1	2.7 ± 0.9	2.2 ± 1.2
Spleen (7)			
Total T	19.6 ± 4.4	18.5 ± 2.3	23.3 ± 4.9
CD4$^+$CD8$^-$	12.0 ± 2.9	11.8 ± 1.6	14.7 ± 3.4
CD4$^-$CD8$^+$	7.5 ± 1.7	6.7 ± 0.9	8.5 ± 1.8
Lymph nodes (4)			
Total T	3.7 ± 1.2	1.9 ± 0.2*	1.9 ± 1.0
CD4$^+$CD8$^-$	2.2 ± 0.7	1.2 ± 0.1*	1.2 ± 0.6
CD4$^-$CD8$^+$	1.5 ± 0.5	0.7 ± 0.1*	0.7 ± 0.4*
Inguinal LNs (16)			
Mean number	2.0	1.8	0.7**
Mean volume	3.4 ± 1.7	2.0 ± 0.9*	1.2 ± 0.6**
Peyer's Patches (5–7)			
Mean number	6.5	6.4	1.7**
Aggregate volume (mm^3)	30.3 ± 8.8	17.8 ± 4.3**	2.3 ± 1.7**

Numbers in parentheses refer to the number of mice analyzed for the values shown. Significance at *p < 0.05 or **p < 0.01.
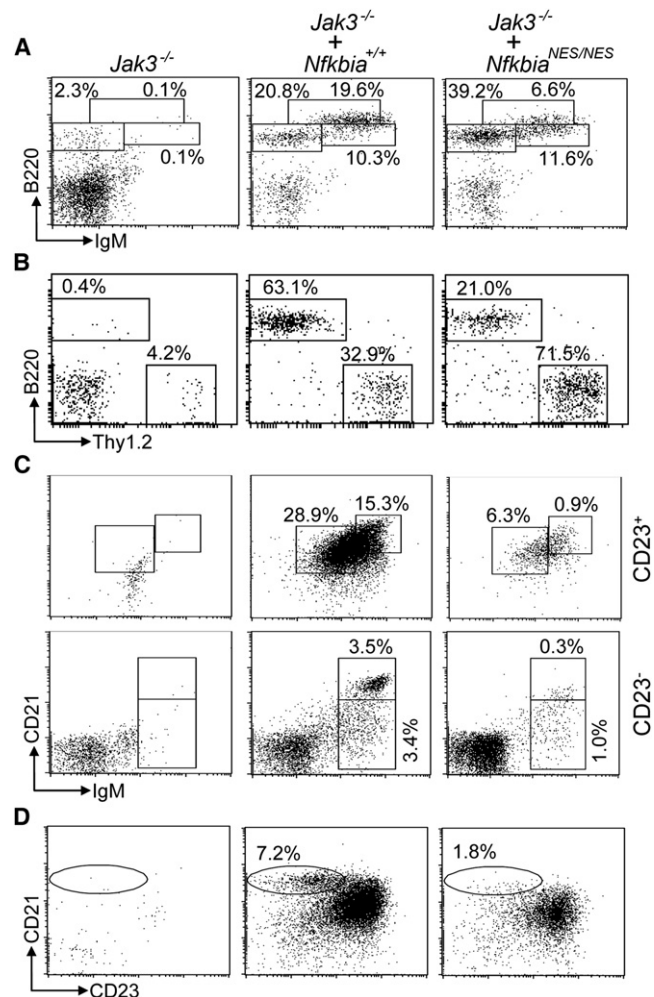

Figure 3. Severely Impaired B Cell Maturation in Recipients of BM from *Nfkbia*$^{NES/NES}$ Mice

Sublethally irradiated *Jak3*$^{-/-}$ mice were transplanted with BM from WT (*Jak3*$^{-/-}$ + *Nfkbia*$^{+/+}$) or *Nfkbia*$^{NES/NES}$ (*Jak3*$^{-/-}$ + *Nfkbia*$^{NES/NES}$) mice. Irradiated *Jak3*$^{-/-}$ mice without BM transplantation were used as a negative control.

(A) BM from the recipient mice were stained with anti-B220 and anti-IgM. Percentages here and below indicate cells in the gated lymphoid population.

(B) Splenocytes from the recipients were stained with anti-B220 and anti-Thy1.2.

(C) Splenocytes from the recipients were stained with anti-IgM, anti-CD21, and anti-CD23. In cells gated on CD23$^+$, T2 and FO B cells are shown. In cells gated on CD23$^-$, T1 and MZ B cells are shown.

(D) Splenocytes from the recipients were stained with anti-B220, anti-CD21, and anti-CD23. In cells gated on B220$^+$, MZ B cells are shown.

Data are representative of five recipients transplanted with each genotype of BM. Controls in (C) and (D) are not shown due to very low percentages.

expression of target genes associated with these processes, and B cell maturation defects at the T$_1$-T$_2$ transition are all consistent with this model.

In contrast to the defects of B cell maturation, the abnormal formation of the spleen, inguinal lymph nodes (LN), and Peyer's patches (PP) observed in *Nfkbia*$^{NES/NES}$ mice have not been reported in *Rel*$^{-/-}$ or *Rel*$^{-/-}$*Nfkb1*$^{-/-}$ mice (Köntgen et al., 1995; Pohl et al., 2002). The proper development of LN and PP requires the convergence of both canonical and noncanonical NF-κB activation pathways through a combined action of lymphotoxin (LT)α$_1$β$_2$-LTβ receptor (R), tumor necrosis factor (TNF) α, or LTα$_3$-TNFR1, and receptor activator of nuclear factor

kappa-B ligand (RANKL-RANK) pathways (Drayton et al., 2006; Hoffmann and Baltimore, 2006; Weih and Caamaño, 2003). In contrast to *Nfkb1*$^{NES/NES}$ mice, *Rankl*$^{-/-}$ and *Rank*$^{-/-}$ mice show LN defects but the PP development and spleen architecture are largely normal (Dougall et al., 1999; Kong et al., 1999). Similarly, *Tnfr1*$^{-/-}$ and *Traf2*$^{-/-}$ mice show PP defects but have normal LNs and spleen (Piao et al., 2007), again differing from *Nfkbia*$^{NES/NES}$ mice. Finally, *Ltα*$^{-/-}$ and *Ltβr*$^{-/-}$ mice lack
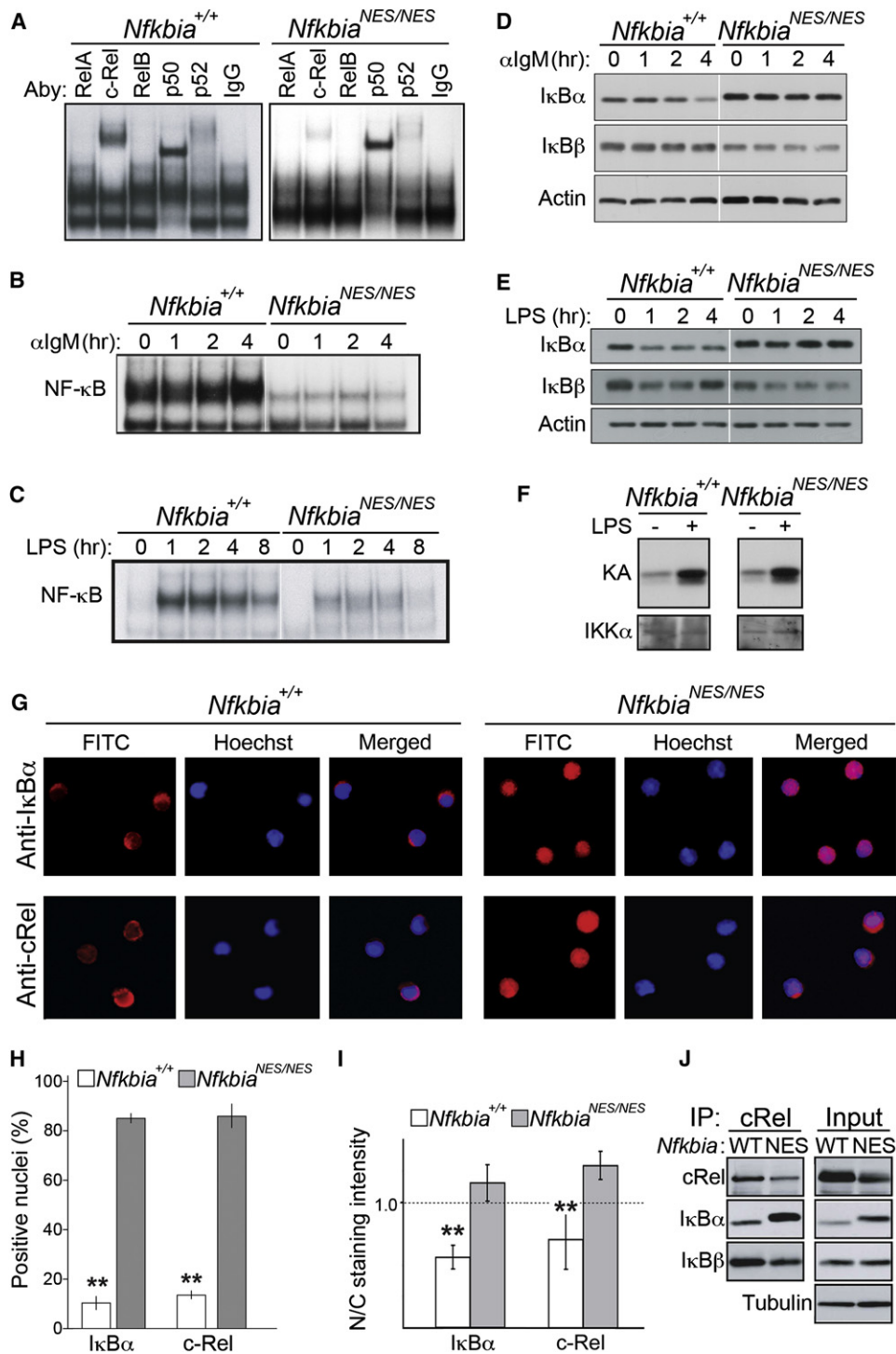
Figure 4. Defects in NF-κB Activation and cRel and IκBα Localization in Nfkbia^NES/NES B Cells

(A) Total cell lysates of unstimulated splenic AA4.1⁻ mature B cells from WT and *Nfkbia*^NES/NES mice were analyzed by a supershift assay to detect different NF-κB family members.

(B and C) Splenic AA4.1⁻ mature B cells of WT and *Nfkbia*^NES/NES mice were stimulated with anti-IgM (10 μg/mL, B) and LPS (10 μg/mL, C) for the indicated times. Total cell extracts were made and NF-κB activity was measured by EMSA with an Igκ-κB probe. Variable increases in p50 homodimer binding seen in (B) are probably due to enhanced detection of p50 homodimer that has a lower affinity to the Igκ-κB site used because of the lack of competition by high-affinity heterodimer complexes for a limited amount of probe used. A short exposure time is shown in (C) to highlight the difference of induced activity (the basal activity difference is thus less evident because of underexposure).

(D and E) Samples in (B) and (C) were analyzed by immunoblotting with anti-IκBα, -IκBβ, and -actin.

all LN and PP and exhibit a disorganized spleen (Banks et al., 1995; De Togni et al., 1994) whereas $Lt\beta^{-/-}$ mice lack peripheral LN and PP but retain mesenteric and cervical LN (Koni et al., 1997). $Lt\alpha^{-/-}$ and $Lt\beta^{-/-}$ mice also show a reduction in serum IgA (Koni et al., 1997) similar to that seen in $Nfkbia^{NES/NES}$ mice, consistent with the role of mucosal lymphoid organs, such as PPs, as the predominant producers of IgA (Kelsall, 2008). Clues to why $Nfkbia^{NES/NES}$ mice have defective LN organogenesis confined to the inguinal LNs may lie in the fact that development of LN groups requires distinct amounts of signaling as highlighted by mice deficient in LTα, LTβ, and LTβR (Banks et al., 1995; De Togni et al., 1994; Koni et al., 1997). Thus, both canonical and noncanonical NF-κB functions in critical cell types, including B cells, are probably sufficiently perturbed in $Nfkbia^{NES/NES}$ mice to induce the observed secondary lymphoid organ and tissue defects that were not observed in $Rel^{-/-}$ or $Rel^{-/-}Nfkb1^{-/-}$ mice.

Unlike defects in B cells and secondary lymphoid organs and tissues, based on CD4 and CD8 cell surface staining alone we did not observe perturbations in CD4$^+$ and CD8$^+$ thymic T cell development or their numbers in thymus and spleen of the $Nfkbia^{NES/NES}$ mice. In T cells, it is reported that IκBα is mostly associated with RelA, not cRel (Sen, 2006; Tam et al., 2001). RelA, but not cRel or p50, harbors an intrinsic NES motif (Harhaj and Sun, 1999; Tam et al., 2001). Accordingly, subcellular localization of inactive RelA complexes in $Nfkbia^{NES/NES}$ thymic and splenic T cells was mostly cytoplasmic even though a complex between RelA and mutant IκBα could be readily detected. Thus, it appears that the RelA NES compensated for the lack of nuclear export function in NES mutant IκBα. However, consistent with recent reports demonstrating the role of cRel in the development of regulatory T cells (Deenick et al., 2010; Hori, 2010; Isomura et al., 2009; Long et al., 2009; Ruan et al., 2009; Vang et al., 2010; Visekruna et al., 2010; Zheng et al., 2010), we found evidence for developmental defects of this cell type in $Nfkbia^{NES/NES}$ mice. In addition, CD4$^+$ but not CD8$^+$ memory-like T cells in the mutant mice were also reduced, consistent with previous reports on the role of cRel and p50 in the development of CD4$^+$ memory-like T cells (Zeng et al., 2008; Zheng et al., 2003). Therefore, molecular defects arising from defective IκBα export also impinge on these T cell subsets and more analyses are warranted to fully investigate molecular, biological, and pathological consequences of reduced regulatory and memory-like T cells in $Nfkbia^{NES/NES}$ mice.

In conclusion, derivation and analysis of $Nfkbia^{NES/NES}$ mice revealed the surprisingly widespread role for IκBα N-NES in vivo. To our knowledge, $Nfkbia^{NES/NES}$ mice represent the first in vivo model to directly evaluate the role of a specific NES motif in the regulation of the NF-κB-Rel family of transcription factors. Other mechanisms that control subcellular distribution of NF-κB-Rel proteins, including RelA NES, IκBα C-NES, and IκBε NES, could also play important roles in a cell type- or context-dependent manner. Resolving in vivo roles of these discrete mechanisms will necessitate creation and analysis of additional animal models. Similarly, although nucleocytoplasmic regulation mediated by specific NES motifs has been documented for many other critical regulatory factors, including the tumor suppressor p53 (Chu et al., 2007; Terry et al., 2007), direct examination of the functions of most of these NES-mediated export mechanisms in vivo remain to be performed. Additional in vivo studies in which specific NES motifs are disrupted will help broaden our understanding of the control of biological and pathological processes via active nuclear export of regulatory factors.

EXPERIMENTAL PROCEDURES

Generation of $Nfkbia^{NES/NES}$ Mice

In brief, the targeting construct harboring a genomic $Nfkbia$ locus with the triple IκBα N-NES mutation (M45A,L49A,I52A) introduced within exon 1 was electroporated into 129/Sv R1 ES cells. Two correctly targeted ES cell clones (11D and 12G clones; Figure S1B) were each injected into C57BL/6J blastocysts to generate chimeras. Germline-transmitted $Nfkbia^{+/NES}$ lines were then generated and subsequently crossed with EIIa-cre mice to delete the neo cassette in germline (Lakso et al., 1996), and the mice with mutant $Nfkbia$ allele lacking both the neo cassette and the EIIa-cre gene were backcrossed onto the C57BL/6J strain for 5–7 generations. Two independent $Nfkbia^{+/NES}$ lines were derived from the original two ES clones. The bulk of the data presented is derived from the analysis of 11D mouse line. Similar results were also confirmed in a limited analysis of the 12G line. See Supplemental Experimental Procedures for further details.

Lymph Node and Peyer's Patch Analyses

Inguinal LNs were enumerated in situ by visual examination. LN volume was derived from the formula width^2 × length/2 of histologic sections. PPs were enumerated by visual examination of flushed small bowels. The aggregate volume of PPs in each mouse was determined by the sum of estimated volumes for each PP as above.

Flow Cytometry

Single-cell suspensions from BM, spleen, and lymph nodes were treated with Gey's solution to lyse red blood cells and then resuspended in phosphate-buffered saline (PBS) with 2% fetal bovine serum (FBS). The cells were stained with a combination of fluorescence-conjugated antibodies. Allophycocyanin (APC)-conjugated anti-B220 (17-0452), anti-IgM (17-5790-82), anti-CD4 (17-0042-82), fluorescein isothiocyanate (FITC)-conjugated anti-Thy1.2 (11-0902), anti-BAFFR (11-5943), phycoerythrin (PE)-conjugated anti-CD1d (12-0011), and anti-CD9 (12-0091) antibodies and PE-Cy5.5-conjugated

(F) The IKK complex was immunoprecipitated from B cells stimulated with LPS (10 μg/mL for 30 min) and an IKK kinase assay was performed with GST-IκBα(1-66aa) as substrate.

(G) Splenic AA4.1$^-$ mature B cells were fixed and stained with anti-IκBα and anti-cRel and counterstained with Hoechst dye.

(H) Percentages ±1 SD of pronounced nuclear staining for each protein as in (G) were derived from triplicate counts of random 200 cells. **paired t test determined a statistically significant difference p < 0.001.

(I) Quantitation of nuclear and cytoplasmic IκBα and cRel in splenic AA4.1$^-$ mature B cells. Images of stained cells as in (G) were analyzed by Image J software. Mean intensity of staining in the nuclear and cytoplasmic compartments of 10 random cells stained with each antibody, normalized to background intensity, and expressed as a ratio of mean nuclear intensity/mean cytoplasmic intensity (N/C) are shown as columns with 1SD bars. Paired t test determined a statistically significant difference in N/C ratio of IκBα and cRel between WT and mutant cells, **p < 0.001.

(J) Lysates obtained from splenic AA4.1$^-$ mature B cells of WT and $Nfkbia^{NES/NES}$ mice were incubated with anti-cRel and the precipitates were analyzed by immunoblotting with anti-cRel, -IκBα, and -IκBβ (left). Inputs were blotted with the same antibodies and an anti-tubulin loading control (right).

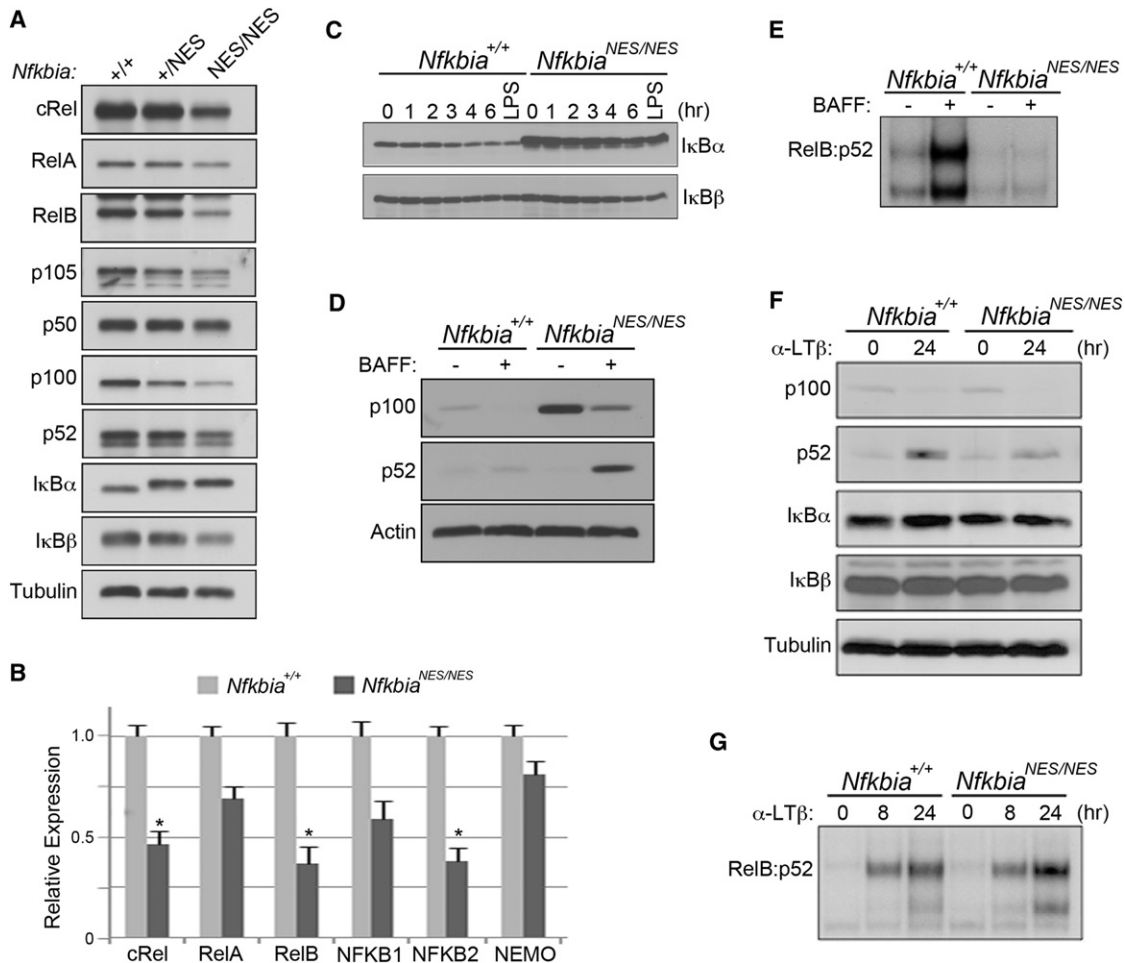**Figure 5. Reduced Expression of Noncanonical NF-κB Members and Activation in *Nfkbia*[NES/NES] B Cells**

(A) Splenic AA4.1⁻ mature B cells were purified from *Nfkbia*^{+/+}, *Nfkbia*[+/NES], and *Nfkbia*[NES/NES] mice and total cell extracts were made. The expression of NF-κB and IκB family members were analyzed by immunoblotting.

(B) Total RNA from splenic AA4.1⁻ mature B cells of WT and *Nfkbia*[NES/NES] mice were analyzed by an RT² Profiler Mouse NF-κB Signaling Pathway PCR Array (SA Biosciences) and the statistical analysis was done according to the manufacturer's instructions.

(C) Splenic AA4.1⁻ mature B cells of WT and *Nfkbia*[NES/NES] mice were treated with cycloheximide (25 μg/ml) for indicated times or with LPS alone (10 μg/ml, 1 hr) and total cell lysates were analyzed for IκBα and IκBβ degradation by immunoblotting. The relative degradation as measured by laser scanning of each band followed by NIH ImageJ analysis normalized to actin loading control showed that the rate of mutant IκBα degradation was 2-fold slower than that of the WT protein.

(D) Splenic AA4.1⁻ mature B cells purified from WT and *Nfkbia*[NES/NES] mice were treated with BAFF (500 ng/mL) for 24 hr. The processing of p100 to p52 was detected by immunoblot with an anti-p52.

(E) EMSA analysis was performed with samples in (D) via an Igκ-κB probe.

(F) MEF cells generated from *Nfkbia*[NES/NES] and WT mice were treated with anti-LTβR (0.5 μg/ml) for the indicated times (hr). The processing of p100 was detected by immunoblot with anti-p52 along with antibodies to other NF-κB and IκB family members.

(G) EMSA analysis of extracts from (F) was performed as in (E).

streptavidin (35-4317) were purchased from eBioscience. PE-conjugated anti-B220 (553090), anti-CD43 (553271), anti-CD21 (552957), anti-CD23 (553139), anti-CD5 (01035B), anti-CD8 (553033), APC-conjugated anti-CD19 (550992), FITC-conjugated anti-CD21 (553818), anti-IgD (553439), and biotin-conjugated anti-CD23 (553137) were purchased from BD Biosciences PharMingen. All antibodies were mouse monoclonal antibodies. Apoptosis and cell cycle analyses were done by terminal deoxynucleotidyl transferase dUTP nick end labeling (TUNEL) and propidium iodide (PI) staining (Chen et al., 2008). Samples were applied to a flow cytometer (LSRII, Becton Dickinson). Data were collected and analyzed with CellQuest software (Becton Dickinson).

Bone Marrow Transplantation

Bone marrow (BM) cells were isolated from hind limbs of WT or *Nfkbia*[NES/NES] mice. Subsequently, cells (5 × 10⁶) were injected retroorbitaly into sublethally irradiated (900 rads) *Jak3*^{−/−} recipients as previously reported (Chen et al., 2008). Eight weeks after transplantation, B cell development in the recipients was examined.

Immunocytochemical and Fluorescence Analyses

Tissue sections were stained with tetramethylrhodamine isothiocyanate (TRITC)-conjugated goat anti-mouse IgM (Southern Biotechnology, Birmingham, AL), anti-B220 (BD Bioscience PharMingen), and FITC-conjugated rat
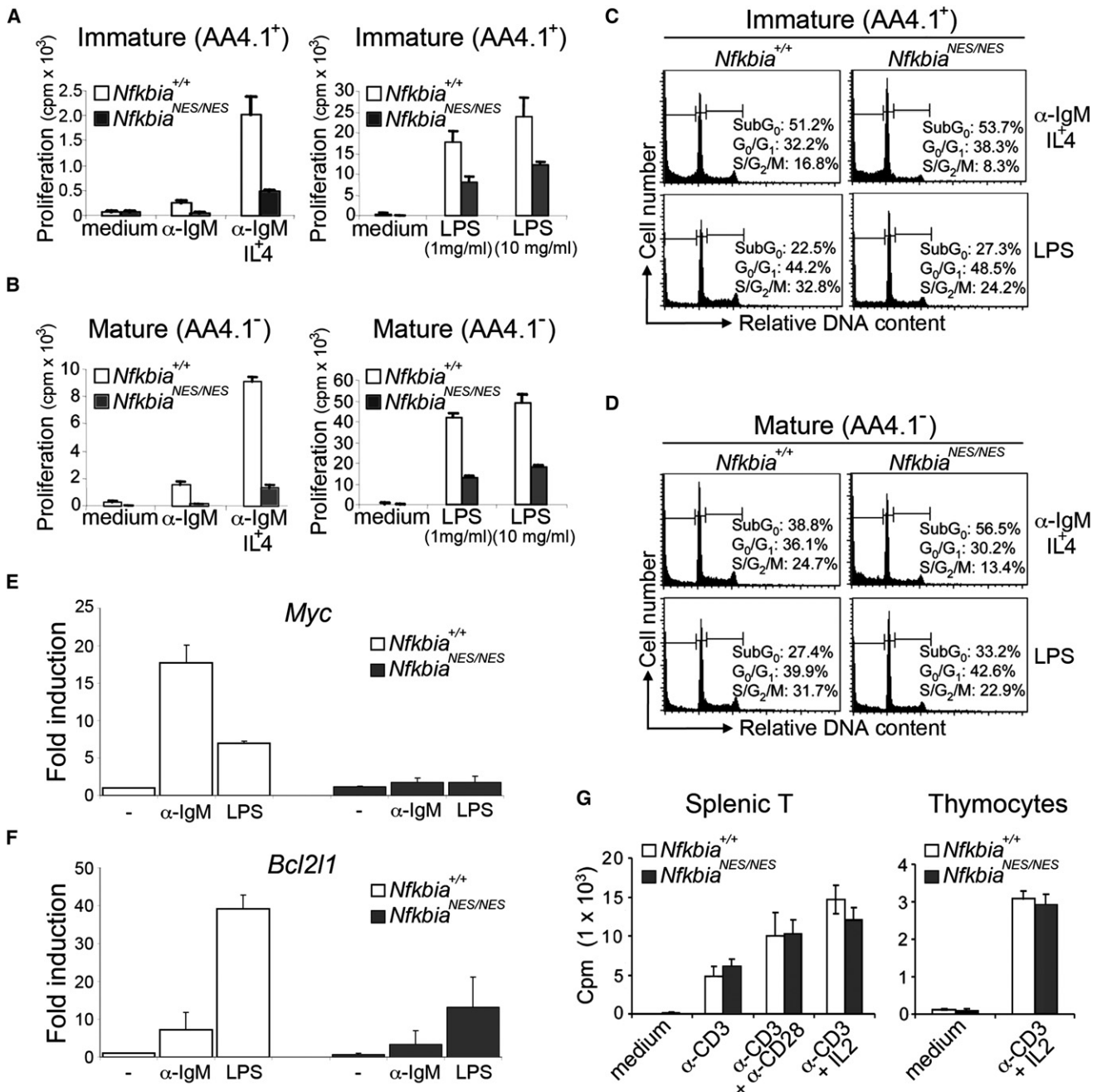
Figure 6. Defective Proliferation and Survival of *Nfkbia*[NES/NES] B Cells

(A and B) Splenic immature (AA4.1[+]) and mature (AA4.1^{−}) B cells purified from WT and *Nfkbia*[NES/NES] mice were stimulated with anti-IgM with or without IL-4 or with LPS. Proliferation was assessed by [³H]thymidine incorporation. Data are representative of at least four independent experiments.

(C and D) Splenic immature (AA4.1[+]) and mature (AA4.1^{−}) B cells were purified from WT and *Nfkbia*[NES/NES] mice and then stimulated with anti-IgM plus IL-4 or with LPS. Subsequently, cells were collected, stained with propidium iodide, and analyzed for cell cycle profile by flow cytometry. The percentages of cells in subG$_0$, G$_0$-G$_1$, and S-G$_2$-M are indicated.

(E and F) Splenic mature (AA4.1^{−}) B cells purified from WT and *Nfkbia*[NES/NES] mice were stimulated with IgM antibody or with LPS. RNA expression amounts of *Bcl2l1* (encoding Bcl-X$_L$) and *Myc* were determined with real-time reverse transcription PCR. Data were done in triplicate from three and two mice each for *Bcl2l1* and *Myc*, respectively.

(G) Spenic and thymic T cells purified from WT and *Nfkbia*[NES/NES] mice were stimulated with indicated agonists and analyzed as in (A).

anti-mouse metallophilic macrophages, MOMA-1 (Serotec), as previously reported (Chen et al., 2008). Images were taken with fluorescence microscope (Zeiss Axioskop, Carl Zeiss Inc., Jena, Germany) with a 10× objective lens

(numerical aperture 0.3) and a charge-coupled device (CCD) camera (Sensys, Photometrics, Tucson, AZ). Alternatively, images were acquired with an Olympus BX41 microscope (Olympus America) and an Olympus DP20

camera, and data were analyzed with the MetaMorph Version 6.1 software (Molecular Devices, Downington, PA).

Analysis of NF-κB and IκBα Subcellular Localization

Splenic B cells were purified by AutoMACS depletion with anti-CD4-, anti-CD8-, and anti-Mac-1-conjugated microbeads (Miltenyi Biotec). The purified cell populations were seeded onto CC2-treated four-well glass chamber slides (Lab-Tek). Cells were stained as in O'Connor et al. (2005). Each experiment was repeated at least twice and 200 cell counts were conducted in triplicate to yield % ± SD.

EMSA, Immunoblotting, and Immunoprecipitation Analyses

Splenic B cells were isolated by negative selection as above. Immature (AA4.1$^+$) and mature (AA4.1$^-$) B cells were separated with biotin-conjugated anti-AA4.1 (eBioscience) and anti-streptavidin microbeads (Miltenyi Biotec). EMSA, immunoblot, and immunoprecipitation analyses were performed as previously described (O'Connor et al., 2004). The antibodies used for immunoblotting were anti-RelA (C-20), anti-RelB (C-19), anti-p52 (C-5), anti-p50 (E-10), anti-IκBα (C-21), anti-IκBβ (C-20), and anti-Actin (I-19) purchased from Santa Cruz Biotechnologies. The cRel antibody (5071) was previously described (Inoue et al., 1991). Anti-tubulin (DM1A) was purchased from Calbiochem.

Proliferation Assay

Cell proliferation was analyzed by ^{3}H-thymidine incorporation assay as previously reported (Chen et al., 2008).

Quantitative RT-PCR and NF-κB Signaling Pathway PCR Array Analysis

See Supplemental Experimental Procedures for details.

SUPPLEMENTAL INFORMATION

Supplemental Information includes Supplemental Experimental Procedures and five figures and can be found with this article online at doi:10.1016/j.immuni.2011.01.014.

REFERENCES

Baeuerle, P.A., and Baltimore, D. (1988). I κ B: A specific inhibitor of the NF-κ B transcription factor. Science 242, 540–546.

Banks, T.A., Rouse, B.T., Kerley, M.K., Blair, P.J., Godfrey, V.L., Kuklin, N.A., Bouley, D.M., Thomas, J., Kanangat, S., and Mucenski, M.L. (1995). Lymphotoxin-α-deficient mice. Effects on secondary lymphoid organ development and humoral immune responsiveness. J. Immunol. 155, 1685–1693.

Carlotti, F., Dower, S.K., and Qwarnstrom, E.E. (2000). Dynamic shuttling of nuclear factor κ B between the nucleus and cytoplasm as a consequence of inhibitor dissociation. J. Biol. Chem. 275, 41028–41034.

Castro, I., Wright, J.A., Damdinsuren, B., Hoek, K.L., Carlesso, G., Shinners, N.P., Gerstein, R.M., Woodland, R.T., Sen, R., and Khan, W.N. (2009). B cell

receptor-mediated sustained c-Rel activation facilitates late transitional B cell survival through control of B cell activating factor receptor and NF-kappaB2. J. Immunol. 182, 7729–7737.

Chen, Y., Yu, M., Podd, A., Wen, R., Chrzanowska-Wodnicka, M., White, G.C., and Wang, D. (2008). A critical role of Rap1b in B-cell trafficking and marginal zone B-cell development. Blood 111, 4627–4636.

Chu, C.T., Plowey, E.D., Wang, Y., Patel, V., and Jordan-Sciutto, K.L. (2007). Location, location, location: Altered transcription factor trafficking in neurodegeneration. J. Neuropathol. Exp. Neurol. 66, 873–883.

De Togni, P., Goellner, J., Ruddle, N.H., Streeter, P.R., Fick, A., Mariathasan, S., Smith, S.C., Carlson, R., Shornick, L.P., Strauss-Schoenberger, J., et al. (1994). Abnormal development of peripheral lymphoid organs in mice deficient in lymphotoxin. Science 264, 703–707.

Deenick, E.K., Elford, A.R., Pellegrini, M., Hall, H., Mak, T.W., and Ohashi, P.S. (2010). c-Rel but not NF-kappaB1 is important for T regulatory cell development. Eur. J. Immunol. 40, 677–681.

Dougall, W.C., Glaccum, M., Charrier, K., Rohrbach, K., Brasel, K., De Smedt, T., Daro, E., Smith, J., Tometsko, M.E., Maliszewski, C.R., et al. (1999). RANK is essential for osteoclast and lymph node development. Genes Dev. 13, 2412–2424.

Drayton, D.L., Liao, S., Mounzer, R.H., and Ruddle, N.H. (2006). Lymphoid organ development: From ontogeny to neogenesis. Nat. Immunol. 7, 344–353.

Fagarasan, S., Watanabe, N., and Honjo, T. (2000). Generation, expansion, migration and activation of mouse B1 cells. Immunol. Rev. 176, 205–215.

Ferch, U., zum Büschenfelde, C.M., Gewies, A., Wegener, E., Rauser, S., Peschel, C., Krappmann, D., and Ruland, J. (2007). MALT1 directs B cell receptor-induced canonical nuclear factor-kappaB signaling selectively to the c-Rel subunit. Nat. Immunol. 8, 984–991.

Ghosh, S., and Hayden, M.S. (2008). New regulators of NF-kappaB in inflammation. Nat. Rev. Immunol. 8, 837–848.

Ghosh, S., and Karin, M. (2002). Missing pieces in the NF-kappaB puzzle. Cell Suppl. 109, S81–S96.

Grumont, R.J., and Gerondakis, S. (1994). The subunit composition of NF-κ B complexes changes during B-cell development. Cell Growth Differ. 5, 1321–1331.

Hardy, R.R., and Hayakawa, K. (2001). B cell development pathways. Annu. Rev. Immunol. 19, 595–621.

Harhaj, E.W., and Sun, S.C. (1999). Regulation of RelA subcellular localization by a putative nuclear export signal and p50. Mol. Cell. Biol. 19, 7088–7095.

Hoffmann, A., and Baltimore, D. (2006). Circuitry of nuclear factor kappaB signaling. Immunol. Rev. 210, 171–186.

Hori, S. (2010). c-Rel: A pioneer in directing regulatory T-cell lineage commitment? Eur. J. Immunol. 40, 664–667.

Huang, T.T., Kudo, N., Yoshida, M., and Miyamoto, S. (2000). A nuclear export signal in the N-terminal regulatory domain of IkappaBalpha controls cytoplasmic localization of inactive NF-kappaB/IkappaBalpha complexes. Proc. Natl. Acad. Sci. USA 97, 1014–1019.

Huxford, T., Huang, D.B., Malek, S., and Ghosh, G. (1998). The crystal structure of the IkappaBalpha/NF-kappaB complex reveals mechanisms of NF-kappaB inactivation. Cell 95, 759–770.

Inoue, J., Kerr, L.D., Ransone, L.J., Bengal, E., Hunter, T., and Verma, I.M. (1991). c-rel activates but v-rel suppresses transcription from κ B sites. Proc. Natl. Acad. Sci. USA 88, 3715–3719.

Isomura, I., Palmer, S., Grumont, R.J., Bunting, K., Hoyne, G., Wilkinson, N., Banerjee, A., Proietto, A., Gugasyan, R., Wu, L., et al. (2009). c-Rel is required for the development of thymic Foxp3+ CD4 regulatory T cells. J. Exp. Med. 206, 3001–3014.

Johnson, C., Van Antwerp, D., and Hope, T.J. (1999). An N-terminal nuclear export signal is required for the nucleocytoplasmic shuttling of IkappaBalpha. EMBO J. 18, 6682–6693.

Kelsall, B. (2008). Recent progress in understanding the phenotype and function of intestinal dendritic cells and macrophages. Mucosal Immunol. 1, 460–469.

Kong, Y.Y., Yoshida, H., Sarosi, I., Tan, H.L., Timms, E., Capparelli, C., Morony, S., Oliveira-dos-Santos, A.J., Van, G., Itie, A., et al. (1999). OPGL is a key regulator of osteoclastogenesis, lymphocyte development and lymph-node organogenesis. Nature 397, 315–323.

Koni, P.A., Sacca, R., Lawton, P., Browning, J.L., Ruddle, N.H., and Flavell, R.A. (1997). Distinct roles in lymphoid organogenesis for lymphotoxins α and β revealed in lymphotoxin β-deficient mice. Immunity 6, 491–500.

Köntgen, F., Grumont, R.J., Strasser, A., Metcalf, D., Li, R., Tarlinton, D., and Gerondakis, S. (1995). Mice lacking the c-rel proto-oncogene exhibit defects in lymphocyte proliferation, humoral immunity, and interleukin-2 expression. Genes Dev. 9, 1965–1977.

Lakso, M., Pichel, J.G., Gorman, J.R., Sauer, B., Okamoto, Y., Lee, E., Alt, F.W., and Westphal, H. (1996). Efficient in vivo manipulation of mouse genomic sequences at the zygote stage. Proc. Natl. Acad. Sci. USA 93, 5860–5865.

Long, M., Park, S.G., Strickland, I., Hayden, M.S., and Ghosh, S. (2009). Nuclear factor-kappaB modulates regulatory T cell development by directly regulating expression of Foxp3 transcription factor. Immunity 31, 921–931.

Malek, S., Chen, Y., Huxford, T., and Ghosh, G. (2001). IkappaBbeta, but not IkappaBalpha, functions as a classical cytoplasmic inhibitor of NF-kappaB dimers by masking both NF-kappaB nuclear localization sequences in resting cells. J. Biol. Chem. 276, 45225–45235.

Nosaka, T., van Deursen, J.M., Tripp, R.A., Thierfelder, W.E., Witthuhn, B.A., McMickle, A.P., Doherty, P.C., Grosveld, G.C., and Ihle, J.N. (1995). Defective lymphoid development in mice lacking Jak3. Science 270, 800–802.

O'Connor, S., Shumway, S.D., Amanna, I.J., Hayes, C.E., and Miyamoto, S. (2004). Regulation of constitutive p50/c-Rel activity via proteasome inhibitor-resistant IkappaBalpha degradation in B cells. Mol. Cell. Biol. 24, 4895–4908.

O'Connor, S., Shumway, S., and Miyamoto, S. (2005). Inhibition of IkappaBalpha nuclear export as an approach to abrogate nuclear factor-kappaB-dependent cancer cell survival. Mol. Cancer Res. 3, 42–49.

Oliver, A.M., Martin, F., Gartland, G.L., Carter, R.H., and Kearney, J.F. (1997). Marginal zone B cells exhibit unique activation, proliferative and immunoglob-ulin secretory responses. Eur. J. Immunol. 27, 2366–2374.

Perkins, N.D. (2007). Integrating cell-signalling pathways with NF-kappaB and IKK function. Nat. Rev. Mol. Cell Biol. 8, 49–62.

Piao, J.H., Yoshida, H., Yeh, W.C., Doi, T., Xue, X., Yagita, H., Okumura, K., and Nakano, H. (2007). TNF receptor-associated factor 2-dependent canon-ical pathway is crucial for the development of Peyer's patches. J. Immunol. 178, 2272–2277.

Pohl, T., Gugasyan, R., Grumont, R.J., Strasser, A., Metcalf, D., Tarlinton, D., Sha, W., Baltimore, D., and Gerondakis, S. (2002). The combined absence of NF-κ B1 and c-Rel reveals that overlapping roles for these transcription factors in the B cell lineage are restricted to the activation and function of mature cells. Proc. Natl. Acad. Sci. USA 99, 4514–4519.

Ruan, Q., Kameswaran, V., Tone, Y., Li, L., Liou, H.C., Greene, M.I., Tone, M., and Chen, Y.H. (2009). Development of Foxp3(+) regulatory t cells is driven by the c-Rel enhanceosome. Immunity 31, 932–940.

Sen, R. (2006). Control of B lymphocyte apoptosis by the transcription factor NF-kappaB. Immunity 25, 871–883.

Stadanlick, J.E., Kaileh, M., Karnell, F.G., Scholz, J.L., Miller, J.P., Quinn, W.J., 3rd, Brezski, R.J., Treml, L.S., Jordan, K.A., Monroe, J.G., et al. (2008). Tonic B cell antigen receptor signals supply an NF-kappaB substrate for prosurvival BLyS signaling. Nat. Immunol. 9, 1379–1387.

Tam, W.F., Lee, L.H., Davis, L., and Sen, R. (2000). Cytoplasmic sequestration of rel proteins by IkappaBalpha requires CRM1-dependent nuclear export. Mol. Cell. Biol. 20, 2269–2284.

Tam, W.F., Wang, W., and Sen, R. (2001). Cell-specific association and shut-tling of IkappaBalpha provides a mechanism for nuclear NF-kappaB in B lymphocytes. Mol. Cell. Biol. 21, 4837–4846.

Terry, L.J., Shows, E.B., and Wente, S.R. (2007). Crossing the nuclear enve-lope: hierarchical regulation of nucleocytoplasmic transport. Science 318, 1412–1416.

Thomis, D.C., Gurniak, C.B., Tivol, E., Sharpe, A.H., and Berg, L.J. (1995). Defects in B lymphocyte maturation and T lymphocyte activation in mice lack-ing Jak3. Science 270, 794–797.

Vallabhapurapu, S., and Karin, M. (2009). Regulation and function of NF-kappaB transcription factors in the immune system. Annu. Rev. Immunol. 27, 693–733.

Vang, K.B., Yang, J., Pagán, A.J., Li, L.X., Wang, J., Green, J.M., Beg, A.A., and Farrar, M.A. (2010). Cutting edge: CD28 and c-Rel-dependent pathways initiate regulatory T cell development. J. Immunol. 184, 4074–4077.

Visekruna, A., Huber, M., Hellhund, A., Bothur, E., Reinhard, K., Bollig, N., Schmidt, N., Joeris, T., Lohoff, M., and Steinhoff, U. (2010). c-Rel is crucial for the induction of Foxp3(+) regulatory CD4(+) T cells but not T(H)17 cells. Eur. J. Immunol. 40, 671–676.

Weih, F., and Caamaño, J. (2003). Regulation of secondary lymphoid organ development by the nuclear factor-kappaB signal transduction pathway. Immunol. Rev. 195, 91–105.

Zeng, H., Chen, Y., Yu, M., Xue, L., Gao, X., Morris, S.W., Wang, D., and Wen, R. (2008). T cell receptor-mediated activation of CD4+CD44hi T cells bypasses Bcl10: An implication of differential NF-kappaB dependence of naïve and memory T cells during T cell receptor-mediated responses. J. Biol. Chem. 283, 24392–24399.

Zheng, Y., Vig, M., Lyons, J., Van Parijs, L., and Beg, A.A. (2003). Combined deficiency of p50 and cRel in CD4+ T cells reveals an essential requirement for nuclear factor kappaB in regulating mature T cell survival and in vivo func-tion. J. Exp. Med. 197, 861–874.

Zheng, Y., Josefowicz, S., Chaudhry, A., Peng, X.P., Forbush, K., and Rudensky, A.Y. (2010). Role of conserved non-coding DNA elements in the Foxp3 gene in regulatory T-cell fate. Nature 463, 808–812.